

## RESEARCH ARTICLE

## Relative Expression of PPAR $\gamma$ and ADIPOQ mRNA as markers of Inhibition Adipogenesis on Mesenchymal Stem Cells after Pulsed Electromagnetic Field (PEMF) Exposure

Puji Sari<sup>1</sup>, Umiatin<sup>2</sup>, Luluk Yunaini<sup>1\*</sup>, Evah Luviah<sup>3</sup>, Nuzli Fahdia Mazfufah<sup>3, 4</sup>

<sup>1</sup>. Department of Medical Biology, Faculty of Medicine, Universitas Indonesia, Indonesia.

<sup>2</sup>. Department of Physics, Universitas Negeri Jakarta, Indonesia.

<sup>3</sup>. Stem Cells and Tissue Engineering Research Center, IMERI, Faculty of Medicine, Universitas Indonesia, Indonesia.

<sup>4</sup>. Master Program of Biomedical Sciences, Faculty of Medicine, Universitas Indonesia, Indonesia.

**\*Corresponding Author: Luluk Yunaini**

### Abstract

**Objective:** Obesity has become a major health problem in the world. PEMF is a modality for healing obesity because its ability to inhibit adipogenesis. Adipogenesis involves PPAR $\gamma$  transcription factor which plays a role in activating adipogenic genes, including ADIPOQ. PPAR $\gamma$  is highly expressed in the early stages of adipogenesis and ADIPOQ is highly expressed in the termination phase of adipogenesis. Both of these genes can be used as a marker of adipogenesis. This study aimed to determine the level of PPAR $\gamma$  and ADIPOQ expression in the group of MSCs that were exposed to PEMF and the group of MSCs that were not exposed to PEMF. **Methods:** The MSCs were exposed with PEMF intensity of  $B_{max} = 2$  mT,  $f = 75$  Hz, 10 minutes a day for 14 days. Total RNA was extracted from MSCs from each treatment group on day 0 (calibrator), 2, 4, 7, and 14. PPAR $\gamma$  and ADIPOQ mRNA expressions were analyzed using the qRT-PCR method. **Results:** The results of the qRT-PCR analysis showed that the expression of PPAR $\gamma$  and ADIPOQ mRNA in the group that exposed to PEMF was lower than the group of MSCs that were not exposed to PEMF ( $p < 0.05$ ). **Conclusion:** PEMF exposure has an inhibitory effect on adipogenesis of MSCs. PEMF exposure decreased the relative expression of PPAR $\gamma$  and ADIPOQ mRNA.

**Keywords:** PEMF; Adipogenesis; Mesenchymal stem cells; PPAR $\gamma$ , ADIPOQ.

### Introduction

Obesity has become a major health problem throughout the world because it causes various chronic diseases [1]. Obesity is defined as a condition of excessive accumulation of abnormal fat in adipose tissue [2]. Treatment for obese patients has been done by regulating a controlled diet, physical exercise, regulating basic behavior, and the consumption of appetite suppressant drugs [3]. This kind of conventional treatment requires at least one year and sometimes longer to decrease body weight [4]. Based on that data, it is crucial to develop a therapy that is able to increase the opportunities for healing obese patients more efficiently.

One of the modalities that can be used as a therapy for obese patients is therapy using Pulsed Electro-Magnetic Field (PEMF) [5].

The PEMF is a method that uses coils that are fed by dynamic electric current. The dynamic electric current will produce a dynamic magnetic field in the coils but still has non-thermal effect for cells [6]. The changes in the magnetic field will produce an induced electric field on the tissue or cells when exposed to PEMF [7]. The electric field has endogenous mechanisms for cells that will affect resting membrane potential as well as resonance mechanisms in charged the ions transport at the cellular level [7,8].

Magnetic gradient of PEMF can penetrate the cells and changing plasma membrane potential that triggered voltage-gated calcium channels [7, 8]. This can impact the movements of molecules that pass through the plasma membrane, and it can impact the cell activation process such as cell

differentiation [7]. The PEMF has been studied for its effect on inhibiting adipogenesis. Adipocyte cells have a function for energy storage and lipid homeostasis, an imbalance between energy intake and outake on adipose tissue will cause obesity [9]. Observation of the process of adipogenesis can be done in-vivo and in-vitro. As for this study, observations of the process of adipogenesis were carried out in-vitro using Mesenchymal Stem Cells (MSC). MSC is a multipotent cell that can differentiate into several types of cells, including adipocyte cells [10].

In general, adipogenesis is divided into two stages, the first stage is the stage of MSC differentiating to preadipocytes and the next stage is preadipocytes differentiating to mature adipocytes [11]. In culture condition, MSC that are cultured with adipogenic medium are able to complete their differentiation in various time ranges, ranging from 7 to 21 days [12]. Adipogenesis is a very complex process. This process involves several transcriptional factors and intracellular signaling pathways [12]. Peroxisome proliferator-activated receptor gamma (PPAR $\gamma$ ) is a member of the nucleus receptor superfamily as well as a ligand-dependent transcription factor that has functioned as the main regulator of adipocyte differentiation and metabolism [13, 14].

PPAR $\gamma$  carries out its function when forming heterodimers with retinoid X receptors (RXR) and binds to PPAR responsive element (PPRE) on the target gene promoter, which regulates cell differentiation and various metabolic processes, especially lipid and glucose homeostasis [15,16]. PPAR $\gamma$  is highly expressed at the target stage initial differentiation of adipocytes and activated by long chain fatty acids, peroxisomal proliferators, and antidiabetic agent thiazolidinedione [15]. PPAR $\gamma$  overexpression in hemangioma-derived mesenchymal stem is a marker of initiating adipocyte differentiation [17]. In contrast, low expression of PPAR $\gamma$  mRNA in adipose tissue is leads to inhibiting of adipogenesis [18]. Activation of PPAR $\gamma$  induces the activation of adipogenic genes that regulate adipogenesis. One of the main adipogenic genes that being activated by PPAR $\gamma$  is adiponectin (ADIPOQ) [19]. ADIPOQ plays a role in the proliferation and differentiation of preadipocytes into mature adipocytes, increasing the expression

of other genes responsible for adipogenesis, and increasing the lipid content and insulin response from the glucose transport system in adipocytes [20].

A high level of ADIPOQ expression is a marker of the termination and maturation stage of adipogenesis [12]. Overexpressed ADIPOQ in cells will lead to faster adipogenesis [20]. The process of adipogenesis can be assessed by looking at the cell morphology, the number of adipocyte progenitor cells and determining the level of expression of adipogenic genes after stimulation under standard adipogenic conditions [12]. This study aimed to determine the level of PPAR $\gamma$  and ADIPOQ expression in MSCs that were exposed to PEMF and MSCs that were not exposed to PEMF. The results of this study are expected to be a foundational knowledge that can be used in the development of obesity therapy using PEMF devices in the future.

## Materials and Methods

### Culture of Mesenchymal Stem Cell

This experiment used cryopreserved MSCs passage two from Stem Cell and Tissue Engineering Research Center (SCTE-RC), Indonesian Medical Education and Research Institute (IMERI), Faculty of Medicine, Universitas Indonesia. MSCs in this experiment were extracted from donor adipose tissue used Pawitan et al., 2013 isolation method [21].

The donor was a healthy 19-year-old girl. MSCs were taken from the cryopreservation tank and then warmed to a water bath at 37°C. After the thawing process, the cells were moved into a new tube that contained 9 mL of complete medium. The complete medium consisted of 1% antibiotic, 1% antimitotic, 1% glutamine, 1% heparin, 10% serum platelet-rich plasma (PRP), and  $\alpha$ MEM. The cells were centrifuged for ten minutes at 1500rpm/minute. The supernatant was removed, and the pellet was resuspended with 1 mL of complete medium for cell counting.

Cell counts were performed using a hemocytometer by mixing 10  $\mu$ L cells and 10  $\mu$ L trypan blue. Cells ( $3 \times 10^5$  cells) were seeded onto a flask 25 that contained the complete medium and cultured in an incubator at 37°C and 5% CO $_2$ .

The culture medium was changed every three days. When the confluency of the cells reached 100%, the cells were digested with Triple Select and seeded ( $5 \times 10^4$  cells) onto six well culture dishes for the experimental design. According to the experimental design, MSCs were divided into three groups, consisting of one experimental group and two control groups. The experimental group (E) is the MSCs group exposed to PEMF. The first control group (C1) is the MSCs group that is not exposed to PEMF and placed outside the incubator. The second control group (C2) is the MSCs group that is not exposed to PEMF and placed inside the incubator.

### Characterization MSC using Surface Markers Analysis with Flowcytometer

Surface markers analysis was performed using flowcytometer BD FACSARIA™ III (BD Biosciences). MSC were characterized using the following conjugated monoclonal antibody combinations: CD73 PE (phycoerythrin), CD90 FITC (fluorescein isothiocyanate), and CD105 PerCPCy5.5 (phycoerythrin-cyanine 5.5) (BD Biosciences). MSCs ( $5 \times 10^5$  cells) were suspended in PBS and incubated with combinations of the monoclonal antibodies described above.

The cells were put into three different tubes which defined as unstained, isotype, and sample. The unstained tube was a tube that only contained cell samples for control. The isotype used to exclude false positive-negative and to define the baseline. Based on International Society for Cellular Therapy (ISCT) criteria, the MSCs must positively express CD73, CD90, and CD105 [22].

### Characterization MSC using Differentiation Test

Based on International Society for Cellular Therapy (ISCT) criteria, the MSCs must be

able to differentiate into three different lineages such as osteoblasts, chondroblasts, and adipocytes [22]. Cell differentiation testing was carried out using different induction media for each lineage. After cells successfully differentiate, cells fixation using formaldehyde and stained. Osteocyte stained by adding 2% alizarin red pH 4.1-4.3 and incubated for 20 minutes. Chondrocyte stained by adding 1% alcian blue dissolved in 0.1 HCl and incubated for 30 minutes. Adipocyte stained by adding 0.5% oil red o dissolved with 60% isopropanol and incubated for 2-5 minutes. After incubation, cells were rinsed using aquabides and observed under the microscope.

### Induction of Adipogenesis using Adipogenic Differentiation Medium

All the MSCs on the three treatment groups were induced with adipogenic differentiation medium to induced MSCs to differentiate to adipocyte. After MSCs reached 60%- 70% of confluency, the complete medium from MSCs was replaced using adipocyte differentiation medium (StemPro® Adipogenesis Differentiation Kit). The adipogenic induction medium consisted of 1% antibiotic, 1% antimitotic, 10% supplement, and basal medium. The adipogenic induction medium was replaced every three days for 14 days.

### PEMF Exposure

The cells in the control groups were treated without exposure to PEMF. The cells in the experimental group were treated with PEMF for ten minutes per day (the pulse field parameters were as follows: intensity 2 mT, frequency 75 Hz) for 14 days. Cell that exposed to PEMF were placed between two Helmholtz coils of PEMF device (Fig. 1). PEMF device that used in this study refers to study that conducted by Umiatin, 2019 [23].



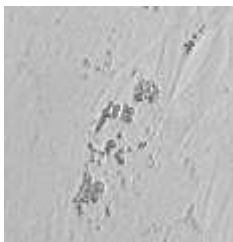

Fig 1: PEMF exposure to MSC

## Morphological Analysis of MSC during Adipogenesis

The morphological analysis aimed to see the characteristics of MSCs from each treatment group during adipogenesis. The characteristics of MSCs were observed based

on the size and the number of fat droplets that formed during adipogenesis. The morphology of MSCs was observed on days 0, 2, 4, 7, and 14 using a microscope. Observation of MSCs morphology during adipogenesis based on the criteria in Table 1 [24].

**Table 1: Cells category during adipogenesis [24]**

Category	Description	Picture
+	The cytoplasm of the cell begins to be filled with small amounts of small lipid droplets	
++	The cytoplasm of the cell begins to be filled with an accumulation of the larger lipid droplets	
+++	The cytoplasm of the cell is filled with single large lipid droplets	Can't find on in-vitro condition.

## RNA Extraction and qRT-PCR Analysis

Total RNA from the three treatment groups was extracted at day 0 (as calibrator), 2, 4, 7, and 14. RNA was extracted using TRIzol™ LS Reagent (Invitrogen, Carlsbad, CA, USA). Calculation of RNA concentration and purity was counted using a spectrophotometer.

The relative expression of PPAR $\gamma$  and ADIPOQ mRNA were detected using qRT-PCR. The relative expression of GAPDH mRNA was used as the control for normalization. The primer sequences were designed using IDT Primer Quest (<https://eu.idtdna.com/>). The primer sequences are shown in Table 2.

**Table 2: Primers used for qRT-PCR**

Gene	Access Code	Nucleotides (5'-3')
PPAR $\gamma$ 2	NM_015869.4	F: GCCTGCATCTCCACCTTATTA R: ATCTCCACAGACACGACATTC
ADIPOQ	NM_001177800.1	F: AGGAGATCCAGGTCTTATTGGTC R: TTCTCCTTTCCTGCCTTGGA
GAPDH	NM_001256799.2	F: CCCTTCATTGACCTCAACTACA R: ATGACAAGCTTCCCCTTCTC

QRT-PCR was performed using Applied Biosystems® 7500 Fast engine and SensiFAST™ SYBR® Lo-ROX One-Step Kit material, which allowed detection of the PCR products by measuring the increase in SYBR green fluorescence caused by the binding of

SYBR green to double-stranded DNA. Each of PCR sample had a volume of 20  $\mu$ L, and the reaction conditions were as follows in Table 3. The relative quantity of mRNA was calculated using the Livak formula ( $2^{-\Delta\Delta C_T}$ ) [25].

**Table 3: Cycle protocol of qRT-PCR**

Cycle	Temperature	Time	Phase
1	45°C	10 min	Activation of the reverse transcription enzyme
1	95°C	2 min	Activation of the polymerase enzyme
40	95°C	5 sec	Denaturation
	55°C	10 sec	Annealing
	72°C	5 sec	Extension

## Statistic Analysis

Statistical analysis was performed using SPSS 22 for Windows. The normality test was performed using the Shapiro-Wilk test. The homogeneity test was performed using the Levene test. The criteria  $p > 0.05$  indicated data is normally distributed and homogeneous. The distribution of data that have normal and homogeneous criteria was continually analyzed by ANOVA test to determine the significance of the parameters between the treatment group and the time of observation. The difference between treatments was then analyzed with Post Hoc Tukey.

If the data is not normally distributed and not homogeneous, then the Kruskal-Wallis non-parametric test was utilized. The differences between the treatments group were then tested with the Mann-Whitney test.

## Results

### Characterization MSC using Surface Markers Analysis with Flowcytometer

The results showed that the MSC positively expressed 97% CD90, 99.2% CD73, and 91.6% CD105.

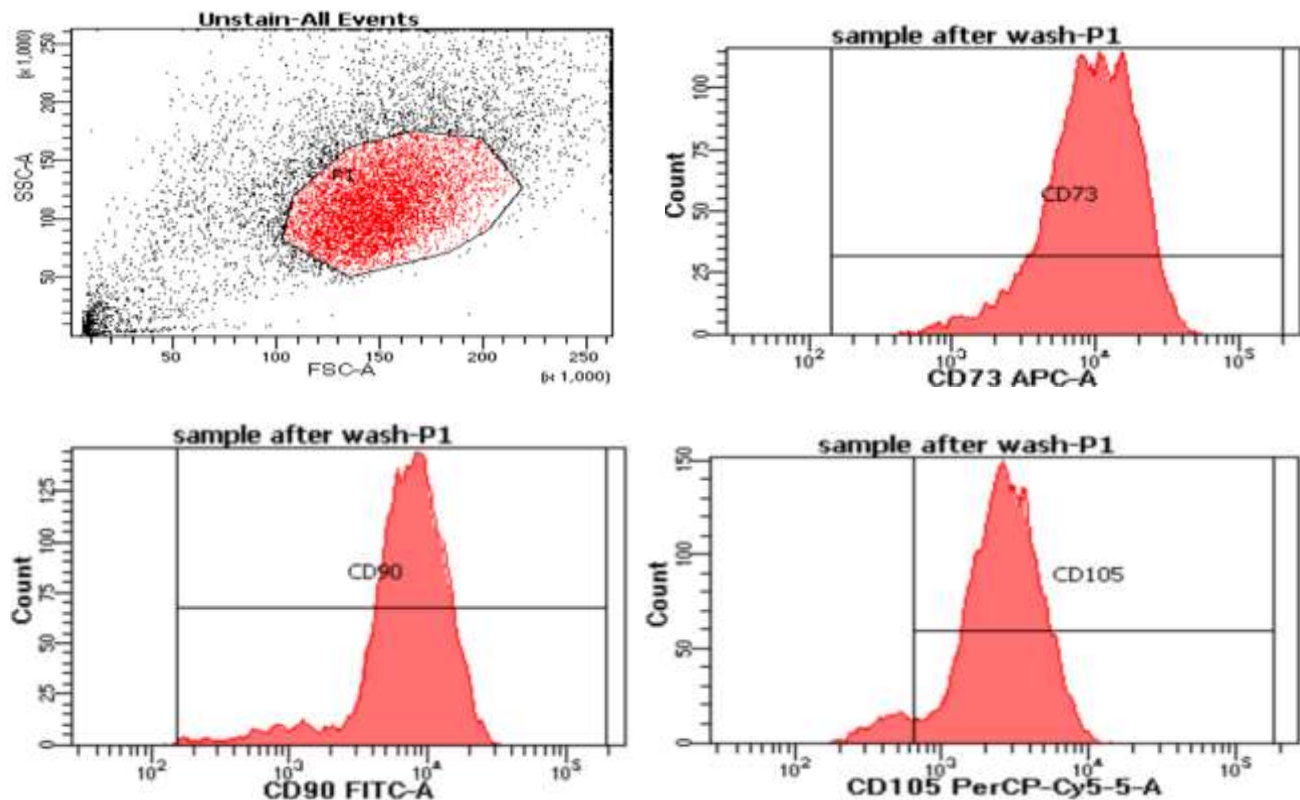


Fig. 3: The results of surface markers analysis using flowcytometer

### Characterization MSC using Differentiation Test

The results of cell staining for each of the differentiation lineage can be seen in Figure 3. In Figure 3a, MSC has successfully differentiated into osteogenic lineage, marked by red coloured cells that came from binding reaction between alizarin red and calcium in the matrix. Figure 3b shows MSC has successfully differentiated into

chondrogenic lineage, marked by blue coloured cells that came from binding reaction between alcian blue and cartilage matrix. Figure 3c shows MSC has successfully differentiated into adipogenic lineage, this is characterized by the formation of lipid droplets that bind to oil red dyes and showed the red color. Based on the results, it can be concluded that MSC used in this study has completed ISCT standard criteria.



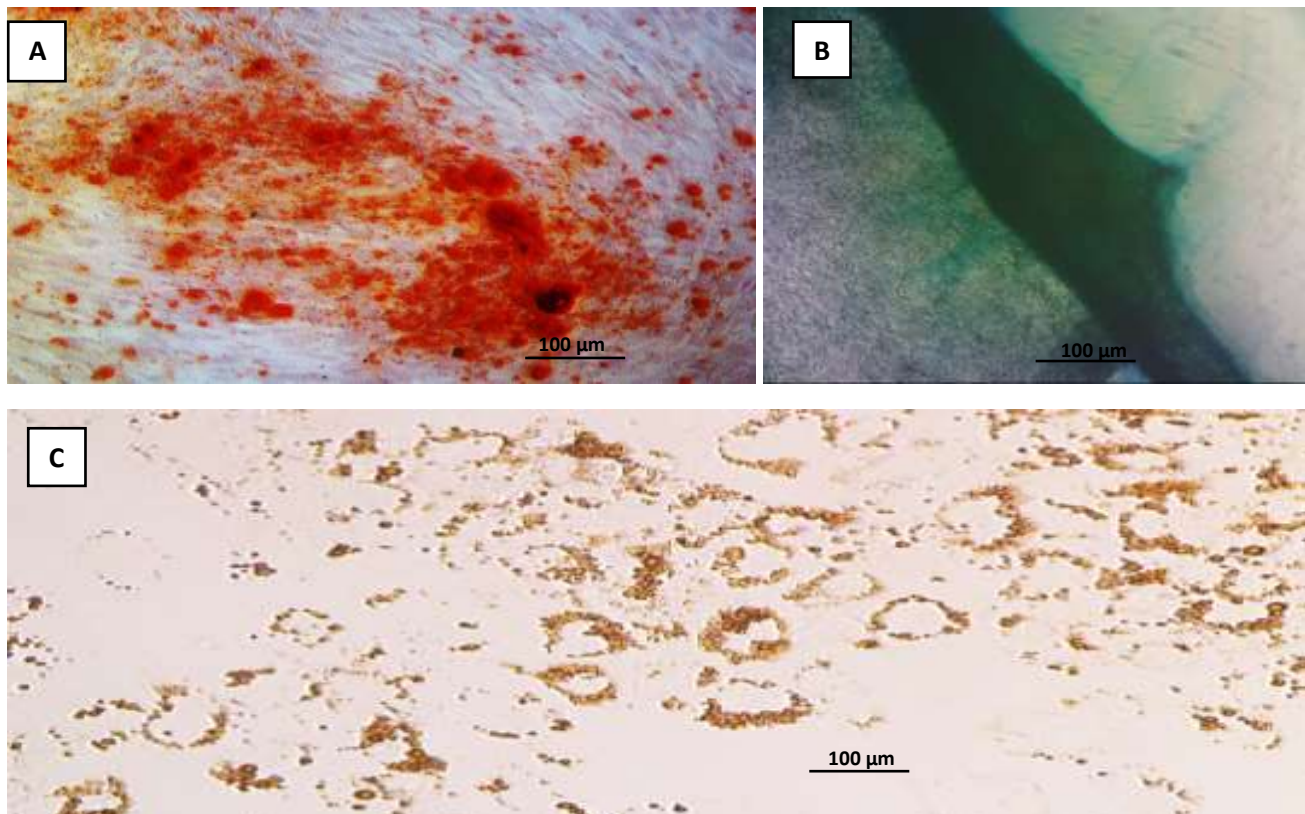


Fig 3: Results of MSC differentiation stained. (a) osteogenic lineage stained with alizarin red; (b) chondrogenic lineage stained with alcian blue; (c) adipogenic lineage stained with oil red o. Picture was taken using microscope with a magnification of 200x

### Morphological Analysis of MSC during Adipogenesis

MSC morphology of the three treatment groups during adipogenesis is shown in

Figure 2. The results of this study indicated that there were morphological differences between the three treatment groups on each day.

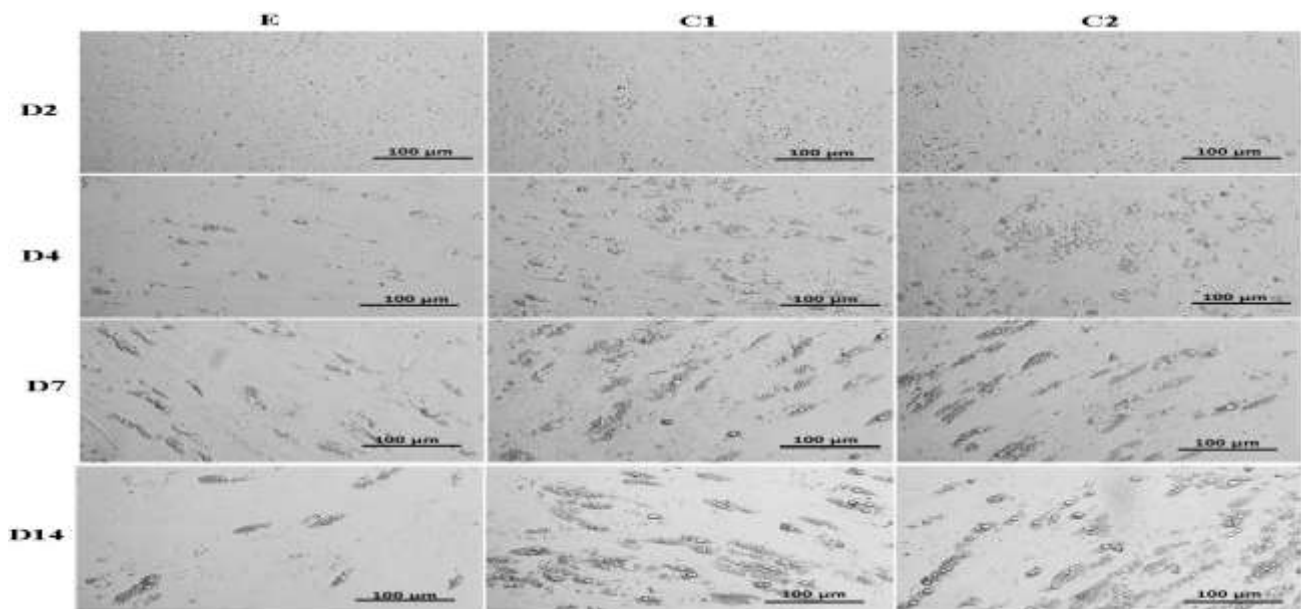


Fig. 4: Comparison of MSCs morphology during adipogenesis. (E: MSC group exposed to PEMF, C1: MSC group that is not exposed to PEMF and placed outside the incubator, C2: MSC group that is not exposed to PEMF and placed inside the incubator; D2: 2nd day, H4: 4th day, H7: 7th day, H14: 14th day). MSC morphology is categorized by categories: (+) cells with small lipid droplets on the cytoplasm, (++) cells with larger lipid droplets on cytoplasm, (+++) cells with single lipid droplets on cytoplasm. In this study there were no cells in the category (+++). Picture was taken using microscope with a magnification of 200x

On day 2, cells with the (+) category, which is the cell with small lipid droplets, appeared to dominate throughout the groups. The cells with (+) category on day 2 indicated that

adipogenesis was entered the initial stage. On days 4 and 7, the number of lipid droplets was getting bigger so that the cells can be classified into categories (++).

On days 4 and 7, the control groups had more cells in the (+) category compared to the PEMF group. On day 14, it was seen that the PEMF group had cells with smaller and fewer lipid droplets compared to the control groups. These results showed that PEMF has an inhibitory effect on the formation of lipid droplets during adipogenesis.

In in-vitro conditions, the characteristics of lipid droplets only can be found in category (+) and (++). Based on the observation, there was no lipid droplet in the category (+++).

These results are the same as the study conducted by Lane et al., 2014. In that study, it was seen that in the early stages of adipogenesis, the cytoplasm of cells began to be filled with small amounts of small lipid droplets. Furthermore, the cytoplasm of cells begins to be filled by the accumulation of rather large-sized fat droplets. But still not found a single lipid droplet that fills the cell (Lane et al., 2014). Table 4 shown the total

number of adipocyte cells that counted manually used images from. The total number of cells was counted based on three categories which previously described in Table 1. On the day 2, it can be seen that the cells formed small lipid droplets on category (+). The number of cells with (+) category in the PEMF group was less than in the two control groups, this difference was statistically different ( $p < 0.05$ ).

On the day 4, it can be seen that the cells formed small lipid droplets on (+) category and cells also founded in the (++) category. The number of cells with (+) and (++) category in the PEMF group was less than in the two control groups, this difference was statistically different ( $p < 0.05$ ). On day 7 and 14, cells with (++) seemed to dominated in two control groups but in the PEMF group, it can be seen that the cells still founded in (+) category. This results shows that PEMF exposure is able to suppress the number of differentiated progenitor adipocyte cells.

**Table 4: The total number of adipocyte-differentiated cells during adipogenesis**

	E (%)			C1 (%)			C2 (%)		
	+	++	+++	+	++	+++	+	++	+++
Day 2	100*	-	-	83	17	-	80	20	-
Day 4	69*	31*	-	55	45	-	51	49	-
Day 7	41*	59*	-	4	96	-	6	94	-
Day 14	30*	70*	-	-	100	-	-	100	-

Note: E: MSC group exposed to PEMF, C1: MSC group that is not exposed to PEMF and placed outside the incubator, C2: MSC group that is not exposed to PEMF and placed inside the incubator. MSC morphology is categorized by categories: (+) cells with small lipid droplets on the cytoplasm, (++) cells with larger lipid droplets on cytoplasm, (+++) cells with single lipid droplets on cytoplasm. In this study there were no cells in the category (+++). (\*) there is a significant difference  $p < 0.05$ , ie between group E with the two control groups on each day

The results of the PPAR $\gamma$  and ADIPOQ mRNA expression are shown in the form of relative expression that compared to the housekeeping gene, GAPDH. A comparison of PPAR $\gamma$  expression based on the treatment group can be seen in Figure 3. Figure 3 showed that PPAR $\gamma$  expression in the PEMF group has a lower level compared to the outside control group and the incubator control group, both on days 2, 4, 7, and 14. After the statistical analysis, a significant difference between the three groups occurred

on day 2 and day 14 of exposure. On day 2 and day 14, significant differences in PPAR $\gamma$  expression occurred between the PEMF group and the outside control group also between the PEMF group and the incubator control group. On day 4 and day 7, there were no statistically significant differences between the three treatment groups. Although in the PEMF group, there was still a lower PPAR $\gamma$  expression compared to the two control groups.

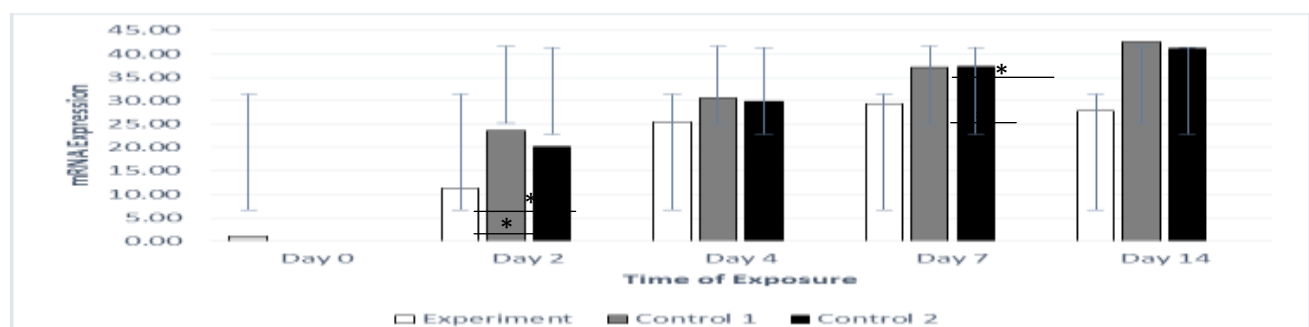


**Fig. 3: PPAR $\gamma$  mRNA relative expression. (\*) indicated that there was a statistically significant difference between the experiment group and control 1, also between the experiment group and control 2 on day 2 and day 14 ( $p < 0.05$ )**

A comparison of ADIPOQ mRNA expression based on the treatment group can be seen in Figure 4. Based on Figure 4, it can be seen that ADIPOQ expression in the PEMF group had a lower level compared to the outside control group and the incubator control group, both on days 2, 4, 7, and 14. After the statistical analysis, a significant difference between the three groups occurred on day 2 and day 14 of exposure. On day 2 and day 14, significant differences in ADIPOQ expression occurred between the PEMF group and the outside control group, also between the PEMF group and the incubator control group. On day 4 and day 7, there were no statistically significant differences between

the three treatment groups. Although in the PEMF group, there was still a lower ADIPOQ expression compared to the two control groups. From the results, it can be seen that the ADIPOQ expression is in line with PPAR $\gamma$  expression. If the PPAR $\gamma$  expression is high, it will be followed by a high ADIPOQ expression and vice versa. The initial phase of adipogenesis is characterized by the induction of PPAR $\gamma$  and C/EBP $\alpha$  [26]. Furthermore, PPAR $\gamma$  and C/EBP $\alpha$  will induce each other through the positive feedback, activation of those transcription factors will continue to the expression of adipogenic target genes during adipogenesis, including ADIPOQ [27].

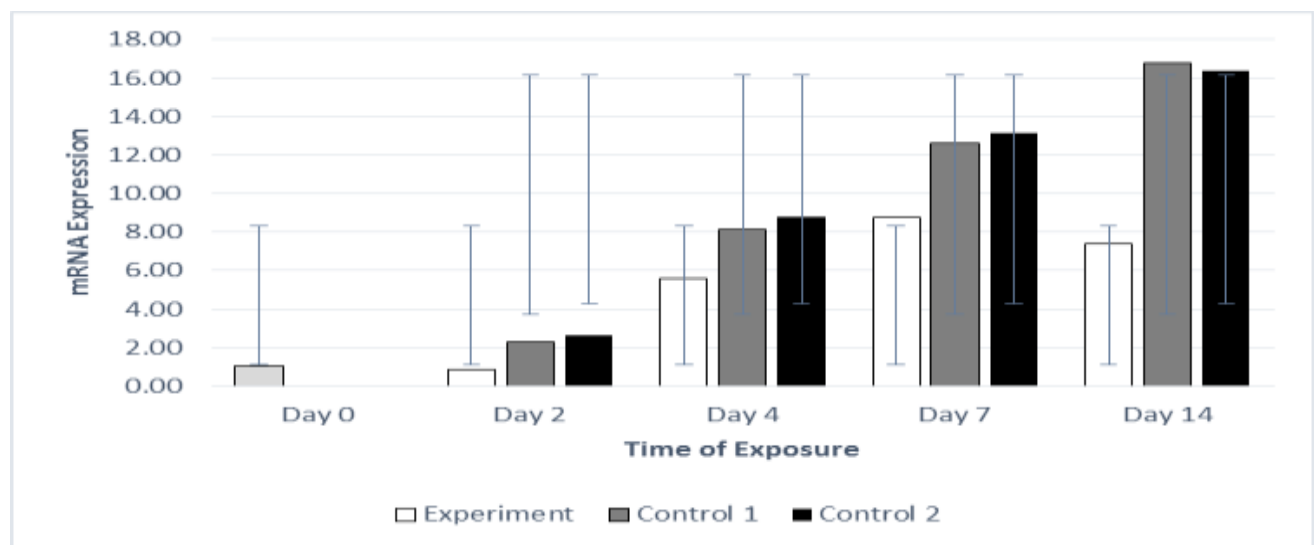


Fig. 4: ADIPOQ mRNA relative expression. (\*) indicated that there was a statistically significant difference between the experiment group and control 1, also between the experiment group and control 2 on day 2 and day 14 ( $p < 0.05$ )

## Discussion

The results showed that exposure to PEMF had a potency to inhibit adipogenesis. The inhibition of adipogenesis showed by decreased expression level of PPAR $\gamma$  that in line with decreased expression level of ADIPOQ. The results of the qRT-PCR analysis showed PPAR $\gamma$  and ADIPOQ expression in the PEMF group lower than the control groups on day 2, 4, 7, and 14.

On day 2, expression level of PPAR $\gamma$  was begun to increased, this recognized as a marker of early stage of adipogenesis. PPAR $\gamma$  is considered as the most powerful transcriptional activator for adipogenesis, so that it is highly expressed during the process of adipogenesis.<sup>16</sup> On day 2, there were significant differences on the expression of PPAR $\gamma$  and ADIPOQ between the PEMF group and the control groups ( $p < 0.05$ ). The PEMF group showed the lower expression level than the other control groups.

On days 4 and 7, the expression of PPAR $\gamma$  and ADIPOQ of the PEMF still lower than control groups but there were no significant differences between the PEMF group and control groups. This was influenced by several factors, including the micro conditions of the cells. It is known that microenvironment contributes to cell differentiation [28].

In this study, cells were cultured in an adipogenic medium that also has an effect to induced the cells to undergo adipogenesis. On day 14, adipogenesis process had to reach the termination stage. In this stage, expression of ADIPOQ was high because it exclusively secreted by mature adipocytes. High level of ADIPOQ expression was found in the final stage of adipogenesis or known as the adipocyte termination and maturation stage.<sup>14</sup> on day 14, the expression of PPAR $\gamma$



still remained high in line with expression of ADIPOQ on the control groups. On the PEMF group, expression of PPAR $\gamma$  and ADIPOQ started to decreased down. The decreased expression of PPAR $\gamma$  and ADIPOQ causes significant differences ( $p < 0.05$ ) between PEMF group and control groups. According to this result, it showed that the time of PEMF exposure has an effect to the inhibition of adipogenesis. From the results, it can be concluded that the electromagnetic stimulus in the form of PEMF is able to inhibit adipogenesis through suppression of PPAR $\gamma$  and ADIPOQ.

The inhibition of adipogenesis with PEMF exposure is supported by research conducted by Du *et al.*, 2015. In this study, the results showed that PEMF exposure with a frequency of 7.5 Hz, magnetic field magnitude 0.4 T, and exposure time 2 hours/day for 15 days of adipogenesis can inhibit the expression of adipogenic genes. However, in this study, the gene expression was only carried out on the last day of exposure, so it could not be seen how the pattern of gene expression occurred during the 15 days of the exposure time.

Inhibition of adipogenesis can be explained by cellular mechanisms but until now, the mechanism still remains unclear. It because the mechanism of PEMF on cells involves complex processes that are needed regarding cross-disciplinary fields. One theory that confirmed the cellular mechanism of PEMF exposure on the cells is the theory of plasma membranes, it is known that PEMF exposure is able to activate voltage-gated ion channels on the plasma membrane that increasing intracellular  $Ca^{2+}$  levels as the mediators for various cellular processes, including proliferation, differentiation and apoptosis of cells [28, 29, 30].

The increasing of cytosolic  $Ca^{2+}$  is triggered by activation of voltage-operated calcium channels (VOCC) and transient receptor potential (TRP) due to the presence of electromagnetic stimulus [31]. This electrical induction is capable of causing changes in membrane polarization, which directly causes the  $Ca^{2+}$  influx through voltage-gated

ion channels [32]. Increasing intracellular  $Ca^{2+}$  activates calmodulin protein which will induce osteogenesis and chondrogenesis but also inhibits adipogenesis [30, 31]. In the role of adipogenesis inhibiting,  $Ca^{2+}$  will bind with calmodulin (CaM) subunit and activates calcineurin (CaN) [32]. This activation will give a specific signal to the nucleus compartment to induce a transcription factor (F1) and block activation of the RXR-PPAR $\gamma$  complex [32]. As a result, the transcription of genes involved in adipogenesis is blocked and adipogenesis does not occur.

Research conducted by Rubio *et al.*, 2018 [33] analyzed the effects of dynamic magnetic field exposure (17-70 mT) on potential changes in the skeletal muscle cell plasma membrane potential. This study confirms that dynamic magnetic fields can induce the eddy current. The eddy current can induce changes in membrane polarization, which leads to the influx of  $Ca^{2+}$  and  $Na^{+}$  through voltage-gated ion channels. The results of this study showed that there is a change in membrane potential 8 mV for 1 second. To reach the threshold for changes in membrane potential, a value of 10-15 mV is required [33].

## Conclusion

PEMF exposure has an inhibitory effect on adipogenesis of MSCs. PEMF exposure decreased the relative expression of PPAR $\gamma$  and ADIPOQ mRNA.

## Acknowledgement

The authors like to thank to Prof. Jeanne Adiwinata Pawitan from Histology Departement, Faculty of Medicine, Universitas Indonesia for technical discussion and Stem Cells and Tissue Engineering Research Center (SCTE-RC), Indonesia Medical Education and Research Institute (IMERI), Faculty of Medicine, Universitas Indonesia for laboratory facilities support. The research was carried out and financially supported by PITTA (International Indexed Publications for UI's Students Final Projects) grant from Universitas Indonesia. This study used for the Master thesis of N.F.M under the supervision of P.J and U.

## References

1. Hruby A, Hu FB (2015) The Epidemiology of Obesity: A Big Picture. *PharmacoEconomics*, 33(7): 673-689. doi:10.1007/s40273-014-0243-x.

2. Longo M, Zatterale F, Naderi J, Parrillo L, Formisano P (2019) Adipose Tissue Dysfunction as Determinant of Obesity-Associated Metabolic Complications, *Int. J. Mol. Sci.* 20: 23-58. doi:10.3390/ijms20092358.
3. Wyatt HR (2013) Update on Treatment Strategies for Obesity. *J. Clin Endocrinol Metab.*, 98(4):1299-1306. DOI: 10.1210/jc.2012-3115.
4. Dwyer JT, Melanson KJ, Sriprachy-anunt U, et al (2000) Dietary Treatment of Obesity. [Updated 2015 Feb 28]. In: Feingold KR, Anawalt B, Boyce A, et al., editors. *Endotext* [Internet]. South Dartmouth (MA): MDText.com, Inc.; Available from: <https://www.ncbi.nlm.nih.gov/books/NBK278991/>.
5. Du L, Fan H, Miao H, Zhao G, Hou Y (2014) Extremely Low Frequency Magnetic Fields Inhibit Adipogenesis of Human Mesenchymal Stem Cells. *Bioelectromagnetics*, 35: 519-530. doi: 10.1002/bem.21873.
6. Sari P, Reihannisha I, Umiatin, Suryandari DA, Yunaini L (2019) Expression relative of RANK, RANKL and OPG gene on rat femoral fracture healing process in delayed union model after pulsed electromagnetic field exposure. *J. Glob. Pharma Technol.*, 11 (4): 223-230.
7. Ross CL (2015) The effect of low-frequency electromagnetic field on human bone marrow stem/progenitor cell differentiation. *Stem Cell Res*, 15: 96-108. doi: 10.1016/j.scr.2015.04.009.
8. Funk RH (2018) Coupling of pulsed electromagnetic fields (PEMF) therapy to molecular grounds of the cell. *Am J. Transl. Res.*, 10(5): 1260-1272. Published 2018 May 15.
9. Dave S, Kaur NJ, Nanduri R, Dkhar HK, Kumar A, et al (2012) Inhibition of Adipogenesis and Induction of Apoptosis and Lipolysis by Stem Bromelain in 3T3-L1 Adipocytes. *PLoS ONE*, 7(1): e30831.
10. Cook D, Genever P (2013) Regulation of mesenchymal stem cell differentiation. *Adv. Exp. Med. Biol.*, (786): 213. doi: 10.1007/978-94-007-6621-1\_12.
11. Dodson MV (2015) Evolution of meat animal growth research during the past 50 years: Adipose and muscle stem cells. *J. Anim. Sci.*, 93: 457-481. doi: 10.2527/jas.2014-8221.
12. Storck K, Ell J, Regn S, Rittler-Ungetüm B, Mayer H, Schantz T, Müller D, Buchberger M (2015) Optimization of in vitro cultivation strategies for human adipocyte derived stem cells, *Adipocyte*. 4(3): 181-187. doi:10.4161/21623945.2014.987580.
13. Lefterova MI, Haakonsson AK, Lazar MA, Mandrup S (2014) PPAR $\gamma$  and the Global Map of Adipogenesis and Beyond. *Trends Endocrinol Metab.*, 25(6): 293-302. doi: 10.1016/j.tem.2014.04.001.
14. Ma X, Wang D, Zhao W, Xu L (2018) Deciphering the Roles of PPAR $\gamma$  in Adipocytes via Dynamic Change of Transcription Complex. *Front Endocrinol (Lausanne)*. 9: 473. doi:10.3389/fendo.2018.00473.
15. Akune T, Ohba S, Kamekura S, Yamaguchi M, Et. Al (2004) PPAR $\gamma$  insufficiency enhances osteogenesis through osteoblast formation from bone marrow progenitors. *The Journal of Clinical Investigation*, 113(6): 846-855.
16. Grygiel-Górniak B (2014) Peroxisome proliferator-activated receptors and their ligands: nutritional and clinical implications - a review. *Nutrition Journal*, 13(17): 1-10.
17. Yuan SM, Guo Y, Wang Q, Xu Y, Wang M (2017) Over-expression of PPAR- $\gamma$ 2 gene enhances the adipogenic differentiation of hemangioma-derived mesenchymal stem cells in vitro and in vivo. *Oncotarget*. (8)70:115817-115828. doi: 10.18632/oncotarget.23705.
18. Kim JH, Lee JH, Park MC, Yoon I, Kim K (2014) AIMP1 negatively regulates adipogenesis by inhibiting PPAR $\gamma$ . *J. Cell Sci.* 127: 4483-4493; doi: 10.1242/jcs.154930.
19. Lowe CE, O'Rahilly S, Rochford JJ (2011) Adipogenesis at a glance. *Journal of Cell Science*. 124: 2681-2686. doi: 10.1242/jcs.079699.
20. Sarjeant K, Stephens JM (2012) Adipogenesis. *Cold Spring Harbor perspectives in biology*, 4(9): a008417. doi:10.1101/cshperspect.a008417.
21. Pawitan JA, Liem IK, Suryani D, Bustami A, Purwoko RY (2013) Simple lipoaspirate washing using a coffee filter. *Asian biomedicine*, 7(3): 333-338.

22. Dominici M, Le Blanc K, Mueller I, Slaper-Cortenbach I, Marini F, Krause D, et al (2006) Minimal criteria for defining multipotent mesenchymal stromal cells. The International Society for Cellular Therapy position statement. *Cytotherapy*, 8(4):315-7.
23. Umiatin, Ismail Hadisoebroto Dilogu, Sastra Kusuma Wijaya, Puji Sari, Andika Dwiputra Djaja (2019) Design and development of pulse electromagnetic fields (PEMF) as adjuvant therapy for fracture healing: A preliminary study on rats. *AIP Conference Proceedings* 2092, 020028 <https://doi.org/10.1063/1.5096696>.
24. Lane JM, Doyle JR, Fortin J, Kopin AS, Orдовás JM (2014) Development of an OP9 Derived Cell Line as a Robust Model to Rapidly Study Adipocyte Differentiation. *PLoS One*, 9(11): e112123. doi: 10.1371/journal.pone.0112123.
25. Livak KJ, Schmittgen TD (2001) Analysis of relative gene expression data using real-time quantitative PCR and the 2<sup>-ΔΔC<sub>T</sub></sup> methods. *Methods*. 25(4): 40-8.
26. Park HS, Ju UI, Park JW, Song JY, Shin DH, Lee KH (2016) PPARγ neddylation essential for adipogenesis is a potential target for treating obesity. *Cell Death Differ.*, 23(8): 1296-1311. doi: 10.1038/cdd.2016.6.
27. Yadollahpour A, Rashidi S (2014) Therapeutic Applications of Electromagnetic Fields in Musculoskeletal Disorders: A Review of Current Techniques and Mechanisms of Action. *Biomedical & Pharmacology Journal*, (7): 23-32. DOI: <http://dx.doi.org/10.13005/bpj/448>.
28. Keung AJ, Kumar S, Schaffer DV (2010) Presentation Counts: Micro environmental Regulation of Stem Cells by Biophysical and Material Cues. *Annu. Rev. Cell Dev. Biol.*, 26: 533-556.
29. Zhang J, Li M, Kang E, Neoh KG (2015) Electrical stimulation of adipose-derived mesenchymal stem cells in conductive scaffolds and the roles of voltage-gated ion channels. 2015. *Acta Biomaterialia*. 32: 46-56. doi: 10.1016/j.actbio.2015.12.024.
30. Brighton CT, Wang W, Seldes R, Zhang G, Pollack SR (2001) Signal Transduction in Electrically Stimulated Bone Cells, *JBJS ORG.* 83-A(10): 1514-1523.
31. Uzielienė I, Bernotas P, Mobasheri A, Bernotienė E (2018) The Role of Physical Stimuli on Calcium Channels in Chondrogenic Differentiation of Mesenchymal Stem Cells, *Int. J. Mol. Sci.*, (1)321-332. doi: 10.3390/ijms19102998.
32. Shi H, Halvorsen Y, Ellis PN, Wilkison WO, Zemel MB (2000) Role of intracellular calcium in human adipocyte differentiation. *Physiol Genomics*, 3(2): 75-82.
33. Rubio AM, Syrovets T, Hafner S, Zablotzki, Dajneka A, Simmet T (2018) Spatiotemporal magnetic fields enhance cytosolic Ca<sup>2+</sup> levels and induce actin polymerization via activation of voltage-gated sodium channels in skeletal muscle cells. *Biomaterials*, 163: 174-184. doi: 10.1016/j.biomaterials.2018.02.031.